Endogenous membrane stress induces T6SS activity in *Pseudomonas aeruginosa*

Anne-Sophie Stolle[a,b], Bradley Thomas Meader[a], Jonida Toska[a], and John J. Mekalanos[a,1]

[a]Department of Microbiology, Harvard Medical School, Boston, MA 02115; and [b]Institute of Infectiology, Center for Molecular Biology of Inflammation, University of Münster, 48149 Münster, Germany

Contributed by John J. Mekalanos, November 19, 2020 (sent for review August 31, 2020; reviewed by Alain Filloux, Samuel I. Miller, and Matthew Parsek)

The type 6 secretion system (T6SS) is a dynamic organelle encoded by many gram-negative bacteria that can be used to kill competing bacterial prey species in densely occupied niches. Some predatory species, such as *Vibrio cholerae*, use their T6SS in an untargeted fashion while in contrast, *Pseudomonas aeruginosa* assembles and fires its T6SS apparatus only after detecting initial attacks by other bacterial prey cells; this targeted attack strategy has been termed the T6SS tit-for-tat response. Molecules that interact with the *P. aeruginosa* outer membrane such as polymyxin B can also trigger assembly of T6SS organelles via a signal transduction pathway that involves protein phosphorylation. Recent work suggests that a phospholipase T6SS effector (TseL) of *V. cholerae* can induce T6SS dynamic activity in *P. aeruginosa* when delivered to or expressed in the periplasmic space of this organism. Here, we report that inhibiting expression of essential genes involved in outer membrane biogenesis can also trigger T6SS activation in *P. aeruginosa*. Specifically, we developed a CRISPR interference (CRISPRi) system to knock down expression of *bamA*, *tolB*, and *lptD* and found that these knockdowns activated T6SS activity. This increase in T6SS activity was dependent on the same signal transduction pathway that was previously shown to be required for the tit-for-tat response. We conclude that outer membrane perturbation can be sensed by *P. aeruginosa* to activate the T6SS even when the disruption is generated by aberrant cell envelope biogenesis.

membrane stress | CRISPRi | T6SS activation | essential gene

The type 6 secretion system (T6SS) is an organelle used by many gram-negative bacteria to inject toxic effector molecules into prokaryotic and eukaryotic cells in a contact-dependent manner (1–10). Some organisms encode one T6SS while others encode multiple systems. For example, *Pseudomonas aeruginosa* carries three T6SS gene clusters encoded by three chromosomal islands, H1, H2, and H3 (3, 11) while *Vibrio cholerae* carries only one (1). All T6SS gene clusters encode a set of conserved proteins that build components typically termed the baseplate, the transmembrane channel, the Hcp tube, the sheath (composed of VipA and VipB in *V. cholerae*) (12), and the trimeric VgrG spike capped by a proline-alanine-alanine-arginine repeat (PAAR) tip as well as several auxiliary proteins that act as effector proteins (4, 5, 13–18). Either spontaneously or after detection of the attack of other bacteria, the spike, tube, and sheath are assembled in a complex that extends from the baseplate and transmembrane channel into the cytosol (4, 5, 14, 19–21). Subsequent contraction of the sheath (termed activation or firing of the T6SS organelle) propels the tube and spike out of the cell through the T6SS transmembrane channel and into extracellular milieu or another nearby cell (5, 14, 22–24). Toxic effector proteins and domains can be fused to spike components, loaded onto the VgrG trimer or PAAR tip with adaptor proteins, or fill the lumen of the Hcp tube (1, 6, 25–34). Delivery of these effector toxins into adjacent cells results in their growth inhibition or death (2, 6, 10, 35). The assembly and firing of the T6SS apparatus can also be visualized by fluorescent fusion constructs, for example to the VipA sheath component (5), while the disassembly of the dynamic organelle can be best visualized by fluorescent fusions to the ClpV T6SS component that disassembles the contracted sheath in typically under 30 s (5).

Different organisms have different strategies for deploying their T6SS. While some strains of *V. cholerae* (e.g., 2740-80 used here) seemingly express their T6SS genes constitutively and then assemble and fire their apparatus in random locations within the cell, *P. aeruginosa* PAO1 uses the T6SS encoded by the H1 locus (the H1-T6SS) (3, 7, 36–41) more defensively by only assembling and firing this organelle precisely where it detects an attack from another nearby bacterium (4, 42, 43). Thus, while *V. cholerae* is efficiently killed in cocultures with *P. aeruginosa* when both organisms contain a functional T6SS, a T6SS negative ($T6SS^-$) *V. cholerae* strain is not killed by *P. aeruginosa* (42). This phenomenon has been coined the T6SS "tit-for-tat" response (42) and has also been observed in the interaction of *P. aeruginosa* with other $T6SS^+$ bacterial species such as *Acinetobacter baylyi* or *Burkholderia thailandensis* (42, 44, 45). Furthermore, *P. aeruginosa* cells that are resistant to their own T6SS attack also display H1-T6SS dynamics similar to the tit-for-tat-like responses; this phenomenon was originally termed "T6SS dueling" (4). This precise assembly and firing of T6SS in two different cells seemingly results in no apparent damage to either of the cells undergoing T6SS dueling, presumably because both sister cells encode immunity proteins to all of the toxic effectors that are delivered (7, 46–48). Thus, the spatially confined, juxtapositioned assembly and firing of the T6SS organelle suggests that a localized activation

Significance

In this study, we applied a CRISPR interference approach to knock down expression of essential genes involved in cell envelope biogenesis and determined if this can trigger *Pseudomonas aeruginosa* T6SS apparatus assembly. We found that disruption of envelope biogenesis can be sensed by the bacteria via a sensory pathway that involves phosphorylation leading to profound T6SS dynamic activation. Our data provide further evidence that membrane disruption is a key signal that drives T6SS organelle assembly. This process likely mimics natural activation pathways that allow *P. aeruginosa* to detect the attack by other aggressive bacteria species and thus sheds further light on the potential key signals that control T6SS organelle biogenesis.

Author contributions: A.-S.S., J.T., and J.J.M. designed research; A.-S.S., B.T.M., and J.T. performed research; A.-S.S., B.T.M., J.T., and J.J.M. analyzed data; and A.-S.S., B.T.M., J.T., and J.J.M. wrote the paper.

Reviewers: A.F., Imperial College London; S.I.M., University of Washington; and M.P., University of Washington.

The authors declare no competing interest.

[1]To whom correspondence may be addressed. Email: john_mekalanos@hms.harvard.edu.

This article contains supporting information online at https://www.pnas.org/lookup/suppl/doi:10.1073/pnas.2018365118/-/DCSupplemental.

Published December 28, 2020.

signal is received by both dueling cells at the precise subcellular localization where effectors are being delivered (4, 42).

P. aeruginosa H1-T6SS activity is also tightly regulated at the transcriptional and translational levels. The Gac/Rsm pathway is involved in control of T6SS through a pathway that involves phosphorylated GacA and induction of the small RNAs *rsmY* and *rsmZ* (38–41, 49, 50). These in turn bind and sequester RsmA, a translational inhibitor of H1-T6SS mRNA. Sequestering of RsmA by *rsmY* and *rsmZ* results in increased translation of the mRNA expressed from the H1-T6SS operon (49). The Gac/Rsm pathway is negatively regulated by RetS and positively regulated by GacS (39). Thus, deletion of *retS* induces the Gac/Rsm pathway and leads to more spontaneous T6SS dueling between sister cells (3, 42).

A second level of T6SS activation control is performed post-translationally by the threonine phosphorylation pathway (TPP) (36, 51–53). It is generally thought that TPP comprises a phosphorylation cascade that transports a signal from the outer membrane protein TagQ (bound to periplasmic TagR) to an inner membrane ABC-transporter-like complex TagTS (52). This signal ultimately leads to expression of the PpkA kinase, phosphorylation of Fha1 of the H1-T6SS locus, and assembly of this T6SS system (36, 52, 53). Dephosphorylation of Fha1 by the PppA phosphatase (51) presumably prevents reassembly of the T6SS organelle and thus returns the cell to its corresponding level of random organelle assembly and firing after ClpV disassembly.

LeRoux et al. (44) have further described a phenomenon called *P. aeruginosa* response to antagonism (PARA), in which transcription of T6SS components is up-regulated upon kin cell lysis through signaling via the Gac-Rsm-RetS signaling pathway. However, the PARA response does not explain how *P. aeruginosa* is able to assemble a H1-T6SS apparatus in a triculture system where it kills T6SS$^+$ *V. cholerae*, but not T6SS$^-$ *V. cholerae* (42). T6SS dueling between homoimmune *P. aeruginosa* sister cells has also been visualized by time-lapse microscopy for both wild type and a *retS* mutant and thus seems unrelated to the PARA response because no cell death is observed during these interactions (4, 6). Thus, it seems most likely that the TagQRST-PpkA-Fha1-PppA signal transduction system is involved in sensing recent T6SS attacks on *P. aeruginosa* cells (42) but how this happens remains to be fully determined. In this regard, it is also interesting that *P. aeruginosa* responds to the conjugative type 4 secretion system (T4SS) of plasmid RP4 by assembling and firing its H1-T6SS apparatus at conjugative donors and that this process also requires the TagQRST-PpkA-FhA1-PppA system (43). Conjugation of RP4 into *P. aeruginosa* clearly must breach the envelope of a recipient cell to deliver DNA without killing the recipient cell but it is unclear how the TagQRST-PpkA-FhA1-PppA system detects this event (43). Chemical substances that interact with gram-negative lipopolysaccharides (LPSs), including polymyxin B (43), DNA, and chelators (54), can also activate the H1-T6SS of *P. aeruginosa* (again dependent on the TagQRST-PpkA-FhA1-PppA system) and these outer membrane perturbants can trigger rapid (i.e., under 1 min) assembly and firing of the H1-T6SS apparatus. Finally, the *V. cholerae* lipase TseL (47) has been reported to be necessary and sufficient to induce the tit-for-tat response by *P. aeruginosa* (55), suggesting that enzymic attack of membrane phospholipids may also trigger the TagQRST-PpkA-FhA1-PppA pathway of H1-T6SS assembly and firing.

In this study, we generated a CRISPR interference (CRISPRi) system for *P. aeruginosa* and used it to knock down essential genes encoding inner membrane, outer membrane, and periplasmic proteins to test if perturbation of cell envelope biogenesis can be sensed by *P. aeruginosa* as a signal to assemble a functional T6SS. We show that the CRISPRi system is functional and efficiently knocks down essential genes resulting in severe growth defects and morphological aberrations in *P. aeruginosa*. We investigated the transcriptional knockdown of *bamA*, *lptD*, and *tolB* in more detail. BamA belongs to the beta barrel assembly machinery (BAM) complex, responsible for insertion of outer membrane proteins (OMPs) into the outer membrane (56–58). LptD transports lipopolysaccharides to the outer leaflet of the outer membrane (59). TolB, one of the most abundant proteins in the periplasm, belongs to the Tol/Pal system and has a role in colicin transport, cell membrane integrity maintenance, and cell division (60–62). We demonstrate that knockdown of *bamA*, *lptD*, and *tolB* results in significantly increased dynamic firing of the H1-T6SS apparatus in a monoculture, suggesting that *P. aeruginosa* is responding to membrane stress with H1-T6SS organelle activation. A knockdown of *bamA* in *P. aeruginosa* also resulted in untargeted aggressive behavior against T6SS$^-$ *V. cholerae*. In a Δ*tagT bamA* knockdown strain, we observed significantly reduced T6SS activity upon CRISPRi knockdown, suggesting that membrane stress caused by aberrant envelope biogenesis can also be sensed by the TagQRST system and triggers the building of a functional T6SS apparatus.

Results

Functional Characterization of a CRISPRi System for *P. aeruginosa*. The CRISPR/Cas9 system is widely known for precisely coordinating double strand breaks in DNA which can powerfully drive genome editing approaches (63, 64). Only two components are needed for a functional CRISPR system: a guide RNA that base pairs target DNA and contains a handle that binds the enzymatic Cas9. Since binding to the target DNA is mediated by base pairing of the RNA, exchange of 20 to 25 base pairs of the guide RNA is sufficient to target a different region in the DNA (63). CRISPR/Cas9 gene editing has revolutionized science in many different fields and is now widely used to generate genetically modified animals and cell lines (64, 65). A variation of the CRISPR/Cas9 technology called CRISPRi allows for transcriptional knockdown of targeted genes (63, 66, 67). By introducing two point mutations in Cas9, which render the enzyme catalytically inactive (dCas9) but preserve its binding capacity to DNA, this system can be repurposed to bind to a target DNA sequence without introducing double strand breaks (63). By directing dCas9 to the promoter region or 3′ end of a gene with a single guide RNA (sgRNA), the CRISPRi system can be used to transcriptionally control target gene expression (66, 67). CRISPRi has been established in several organisms such as *Escherichia coli*, *Lactobacillus plantarum*, *Bacillus subtilis*, *Mycobacterium tuberculosis*, *Streptococcus pneumoniae*, and *V. cholerae* and has been shown to be a useful tool to study essential genes (67–73). The CRISPRi technology is applicable to high-throughput screens as well and has other advantages particularly in the study of essential gene products compared to conventional knockdown methods (67).

In order to establish CRISPRi in *P. aeruginosa*, a gene encoding *dCas9* under the control of an inducible pBAD promoter was integrated into the genome at the phage attachment site *attB* (see *Materials and Methods* for detail). We constitutively expressed an sgRNA targeting each essential gene of interest using a plasmid vector. We found in a survey of a test essential gene (*ftsH*) that CRISPRi knockdown of expression led to a growth defect, while targeting nonessential genes or expressing *dCas9* without a guide showed normal growth (Fig. 1*A*), indicating that the CRISPRi system itself is not toxic to *P. aeruginosa* PAO1 cells. A sgRNA can in theory be targeted to the transcription initiation or elongation regions of a particular gene, as well as either the template or nontemplate strand (Fig. 1*B*) (67). Accordingly, sgRNA guides were designed against these four different regions and their efficacy in target knockdown was measured by qRT-PCR (Fig. 1*C*) as well as the effect of this inhibition on growth (Fig. 1*D*). Targeting the elongation region of the nontemplate strand resulted in the most substantial

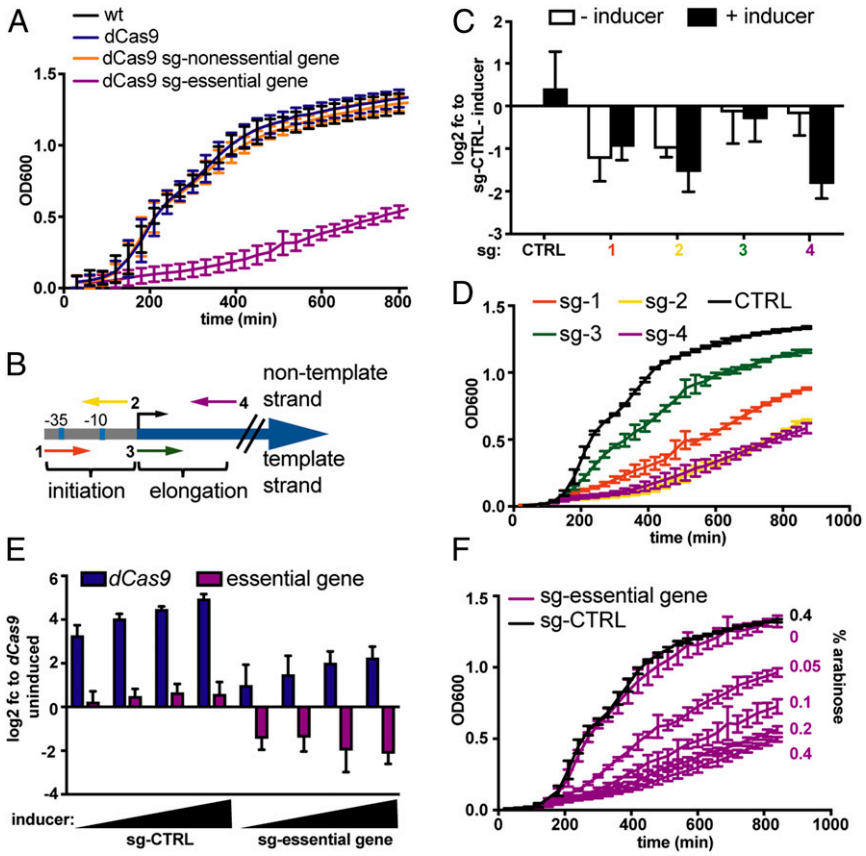

Fig. 1. Essential gene knockdown using CRISPRi. Targeting an essential gene with CRISPRi leads to growth defect. (*A*) Strains were grown in the presence of inducer (0.2% arabinose). OD_{600} was measured every 30 min. (*B*) sgRNA 1 and 2 target the transcription initiation region on the template strand and nontemplate strand, respectively. sgRNA 3 and 4 target the transcription elongation region on the template strand and nontemplate strand, respectively. (*C* and *D*) Sg-1 to 4 targeting an essential gene were tested for target gene knockdown in the presence or absence of inducer in qRT-PCRs (*C*) and growth defect in growth curves. OD_{600} was measured every 30 min (*D*). Knockdown using CRISPRi is dose dependent. Different inducer concentrations were tested for their induction of *dCas9* expression (blue) and efficacy in gene knockdown of an essential gene (purple) in qRT-PCRs (*E*) and growth defect in growth curves. OD_{600} was measured every 30 min (*F*). Graphs display mean ± SD of three independent experiments.

growth defect, so we chose to design all of the following sgRNAs against this region of target genes. Because the CRISPRi we designed is an inducible system, we investigated different concentrations of inducer (0.05 to 0.4% arabinose) on target gene repression (purple) and *dCas9* expression (blue) (Fig. 1*E*) and growth (Fig. 1*F*); transcription and growth phenotypes showed the expected dose–response to up to 0.2% arabinose. Taken together, we show that the CRISPRi system we designed reliably down-regulates transcription of target genes in an inducer dose-dependent manner, is not inherently toxic, and can therefore be used to study essential gene products in *P. aeruginosa* PAO1.

Phenotypic Profiling of *P. aeruginosa* Cells Undergoing Essential Gene Knockdown Using CRISPRi. A set of genes that target essential processes in the periplasm (*lolC* and *tolB*), inner membrane (*ftsH* and *secY*), outer membrane (*bamA* and *lptD*), or the cytosol (*mreB*) in *P. aeruginosa* were selected for further characterization with CRISPRi. Growth curves in microtiter dishes revealed that transcriptional down-regulation of these genes resulted in diminished growth (Fig. 2*A* and *SI Appendix*, Fig. S1 *A–G*). Using flow cytometry, cell death was quantified by measuring percentage of incorporated propidium iodide (PI) over time. After 3 h, the strongest increase in PI uptake was observed for *ftsH* knockdown (Fig. 2*B*). Except for the *secY* knockdown, all knockdowns showed a considerable uptake of PI over time, suggesting that a *secY* knockdown results in bacteriostatic growth arrest, whereas the other knockdowns result in cell lysis to different degrees (*SI Appendix*, Fig. S2 *A–G*). Next, we imaged *P. aeruginosa* strains containing sgCTRL or sgRNA plasmids targeting the essential genes listed above on agarose pads containing 1 μg/mL PI (Fig. 2*C*). The strain expressing sg-*tolB* only showed a growth defect 3 h postinduction (*SI Appendix*, Fig. S1*E*), which is why we analyzed the phenotype of the *tolB* knockdown after 6 h (Fig. 2*D*). We observed striking phenotypic differences that were caused by the knockdown of these essential genes (Fig. 2 *C* and *D*). Knockdown of *bamA* and *mreB* led to rounding up of cells. However, a *bamA* knockdown resulted in smaller round cells than *mreB*. A knockdown in *lolC*, responsible for transport of lipoproteins to the outer membrane, resulted in plasmolysis, whereas *secY* depletion induced a slightly longer cell phenotype than control cells. Knockdown of *tolB* resulted in cells that fail to completely separate upon dividing similar to an observation described by Lo Sciuto et al. (60). Despite a severe growth defect upon knockdown of *lptD* and *ftsH*, we could not observe a severe morphological phenotype in those cells. These targeted essential genes encode inner membrane, outer membrane, or periplasmic proteins and are involved in different pathways that contribute to membrane biogenesis or membrane stability (58, 74–79) and their depletion will ultimately result in membrane stress responses (80–82) in various organisms. Therefore, we determined whether disruption of these different pathways caused different transcriptional stress responses in *P. aeruginosa* PAO1. We transcriptionally profiled an initial group of genes (*bamA*, *lptD*, and *ftsH)* by RNA sequencing (RNAseq)

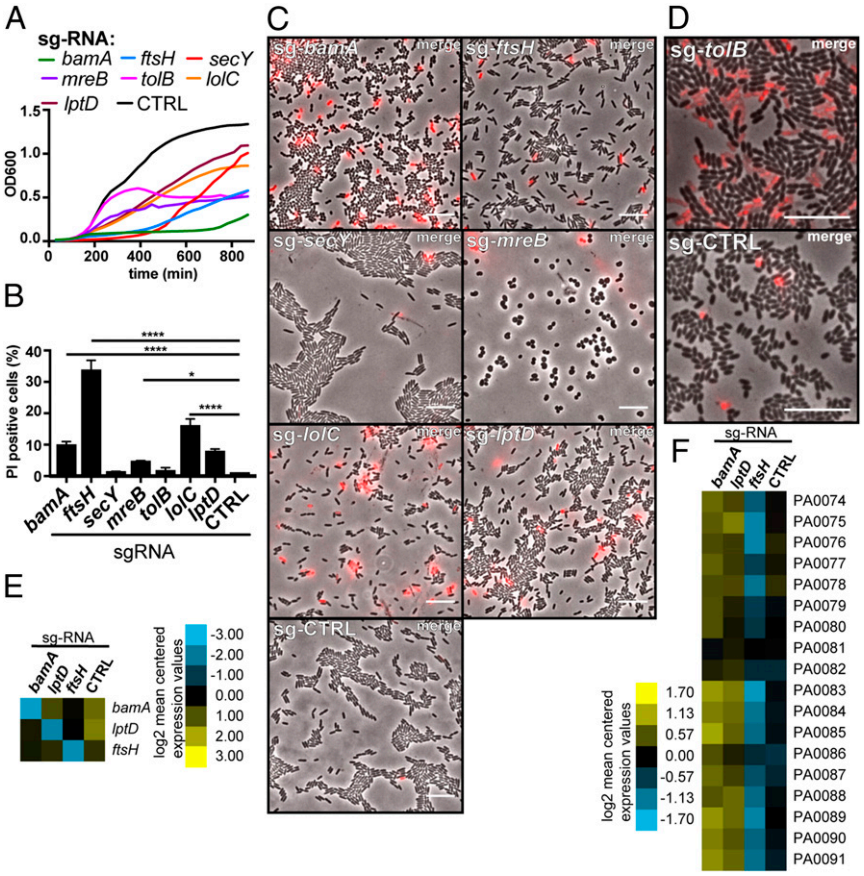

Fig. 2. Gene knockdown of essential genes results in severe growth defects and morphological aberrations. (*A*) Growth curves of *P. aeruginosa* PAO1 strains expressing various sgRNAs grown in microtiter dishes for 15 h in the presence of 0.2% arabinose. The average of three independent biological replicates is displayed. (*B*) Incorporation of PI into *P. aeruginosa* PAO1 strains expressing various sgRNAs after 3 h in the presence of 0.2% arabinose. Graphs display mean ± SD of four independent experiments. $*P < 0.05$, $****P < 0.0001$. (*C* and *D*) *P. aeruginosa* expressing various sgRNAs were grown to midlog (*C*) or early stationary phase (*D*) in the presence of 0.2% arabinose. Strains were imaged in the presence of 1 μg/mL propidium iodide (red) on agarose pads. (Scale bars, 10 μm.) (*E*) Heat map of CRISPRi target transcript levels measured by RNAseq of sg-*bamA*, sg-*lptD*, or sg-*ftsH* knockdown and sgCTRL (each group $n = 3$). (*F*) Heat map of H1 cluster transcript level measured by RNAseq of sg-*bamA*, sg-*lptD*, or sg-*ftsH* and sgCTRL.

(83). We confirmed that knockdown of these targeted essential genes leads to a reduction in the corresponding transcripts (Fig. 2*E* and *SI Appendix*, Fig. S3 *A–C* and Table S4). We observed many responses that were expected to be up-regulated during membrane stress when these genes were knocked down with CRISPRi; these include up-regulation of genes that encode products that include efflux pumps and enzymes involved in modification of lipid A of lipopolysaccharide (Dataset S1 and *SI Appendix*, Tables S8–S13). Even though the pathways that were up-regulated were, in general, not surprising, we could not determine a unique response mechanism to knockdowns of the different selected essential genes (*SI Appendix*, Fig. S3 *A–C* and Tables S8–S13). The transcriptional responses to loss of *bamA* and *lptD* (which encode essential outer membrane proteins) were most similar between the three different knockdown constructs we studied. Knockdown of both of these genes resulted in up-regulation of lipid A modification pathways, isoprenoid catabolic processes, leucine catabolic processes, and extracellular polysaccharide synthesis (*SI Appendix*, Tables S8 and S12). Interestingly, the knockdown of *bamA* and *lptD* also led to increased transcription of H1-T6SS genes (Fig. 2*F* and *SI Appendix*, Fig. S3 *A* and *B* and Table S5), but not the H2 and H3 cluster (*SI Appendix*, Fig. S4 *A* and *B* and Tables S6 and S7). However, knockdown of *ftsH* did not trigger selective up-regulation of H1 (Fig. 2*F* and *SI Appendix*, Fig. S3*C* and Table S5).

Outer Membrane Disruption Leads to Increased T6SS Activity. Since sg-*bamA* and sg-*lptD* resulted in increased transcription of the H1-T6SS gene cluster, we interrogated whether this also resulted in an increase of T6SS activation events in a monoculture of *P. aeruginosa.* Strains containing a ClpV-GFP fusion protein were imaged 3 h post *dCas9* induction on agarose pads. Strains expressing sg-*bamA*, sg-*lptD*, and sg-*tolB* all exhibited increased ClpV-GFP foci (Fig. 3*A*) in comparison to one expressing sgCTRL (representative images are shown in Fig. 3*B*). To confirm that H1-T6SS gene expression is also up-regulated in an sg-*tolB* knockdown, we performed qRT-PCRs on different components of the H1-T6SS cluster. At 3 h, we could not observe an increase in H1-T6SS gene expression (*SI Appendix*, Fig. S5*A*). However, at 5 h, when this strain also displays a growth defect, a clear induction of H1-T6SS genes could be observed for an sg-*tolB* knockdown (*SI Appendix*, Fig. S5*B*). Given that the foci observed represent disassembly of contracted T6SS sheaths (4, 5), we conclude that knockdown of these genes likely increases the level of H1-T6SS activation within the cell population undergoing CRISPRi-mediated transcriptional inhibition.

In general, site-specific binding of the sgRNA-Cas9 (or in our case, dCas9) complex is determined by base pairing of the sgRNA and protospacer adjacent motif (PAM) recognition by Cas9 or dCas9 (63). Hence, mutations in the PAM site lead to loss of binding of the sgRNA-Cas9 or sgRNA-dCas9 complex to its target site and serve as a negative control for specific binding

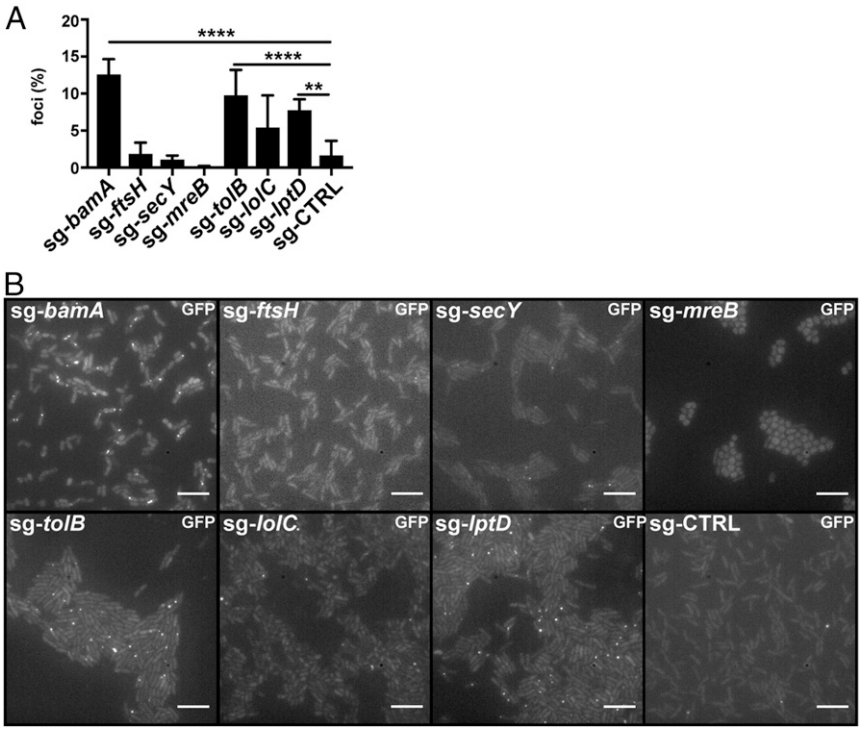

Fig. 3. Knockdown of *bamA, tolB*, and *lptD* leads to increase in T6SS activity. (*A*) Quantification of ClpV-GFP foci in *P. aeruginosa* strains expressing various sgRNA plasmids grown in the presence of 0.1% arabinose. At least 10 different fields per experiment were quantified. Graphs display mean ± SD of three independent experiments. $^{**}P < 0.01$, $^{****}P < 0.0001$. (*B*) Representative images of ClpV-GFP foci in each strain from *A*. (Scale bar, 10 μm.)

of the sgRNA. To confirm that transcriptional repression of one of these genes was responsible for the phenotypes we observed, we elected to mutate the PAM site in the genome of PAO1 *attB*::*dCas9* strain necessary for binding of the dCas9-*bamA* sgRNA complex; this mutation restored gene expression (*SI Appendix*, Fig. S6*A*) and bacterial growth (Fig. 4*A* and *SI Appendix*, Fig. S6*B*) as *bamA* transcription is no longer knocked down. Furthermore, PAM mutation resulted in wild-type levels of T6SS assembly and firing (Fig. 4 *B* and *C*). Thus, the phenotypes observed with a wild-type PAM site expressing dCas9 and sg-*bamA* are likely the result of a specific CRISPRi knockdown of *bamA* transcription.

An increase in ClpV-GFP foci in CRISPRi *bamA*, *lptD*, and *tolB* knockdown strains compared to sgCTRL strains can have

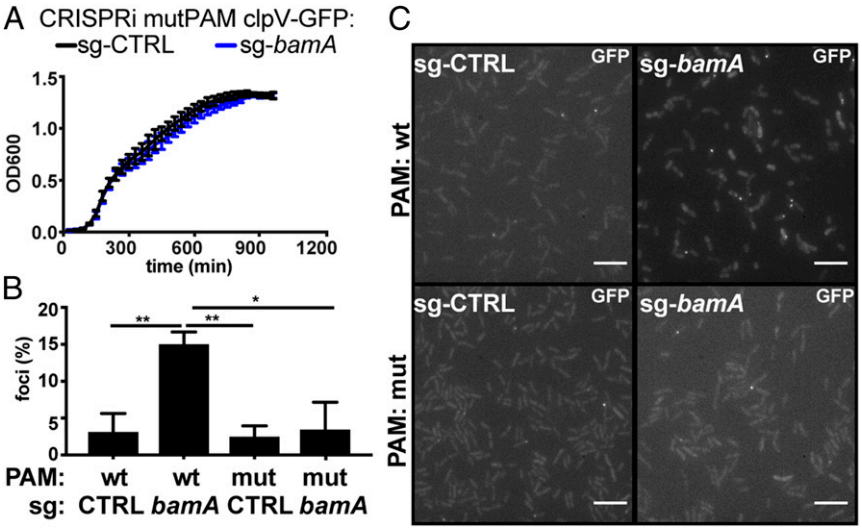

Fig. 4. Restored BamA levels result in normal growth and wild-type T6 activity. (*A*) Strains with mutated PAM sites were analyzed in their growth behavior with sgCTRL or sg-*bamA* guide in a *clpV-gfp* background. Bacteria were grown in the presence of inducer. OD_{600} measurements were taken every 30 min. Graphs display mean ± SD of three independent experiments. (*B* and *C*) Strains were grown to OD 0.7 to 0.85 in the presence of 0.1% arabinose. (*B*) T6SS activity was determined by quantifying ClpV-GFP foci in at least 10 different fields per experiment. Graphs display mean ± SD of three independent experiments. $^{*}P < 0.05$, $^{**}P < 0.01$. (*C*) Representative image of ClpV-GFP imaging of each strain from *B*. (Scale bar, 10 μm.).

different explanations: 1) The T6SS apparatus is locked in its position and cannot be disassembled and hence ClpV-GFP foci accumulate over time, or 2) the average number of T6SS organelles that are assembled and fired is higher in cells undergoing knockdowns of these essential genes. To discriminate between these two possibilities, fluorescent time-lapse imaging was performed. This analysis revealed that *bamA*, *lptD*, and *tolB* knockdown results in dynamic assembly and disassembly of the T6SS apparatus in *P. aeruginosa* cells (Fig. 5*A*, *SI Appendix*, Figs. S7 *A* and *B* and S8 *A* and *B*, and Movies S1–S4). Furthermore, *bamA* knockdown resulted in Hcp secretion (a hallmark of a functional T6SS) in comparison to sgCTRL (Fig. 5*B*). At 0.2% arabinose, we could also observe RNAP accumulation in the supernatant, indicating cell lysis, but at lower concentrations of arabinose, a clear band for Hcp could be detected without RNAP in the supernatant, indicating secretion of Hcp1 via the H1-T6SS apparatus. These results confirm that more functional H1-T6SS nanomachines are built upon knockdown of *bamA* in *P. aeruginosa* PAO1.

TagT Is Required for Enhanced T6SS Organelle Assembly after *bamA* Knockdown. We questioned whether knockdown of *bamA* induces membrane stress that is sensed by the TagQRST-PpkA-FhA1-PppA pathway which is known to drive posttranslational assembly of the H1-T6SS organelle after various exogeneous membrane insults (42, 43, 51–53). Accordingly, we analyzed ClpV-GFP foci formation in a Δ*tagT* knockout background and compared these results to *tagT* wild type in a CRISPRi *bamA* knockdown strain when both strains were also knocked down in *bamA* expression using CRISPRi (Fig. 6 *A* and *B*). These experiments revealed that deletion of *tagT* results in significantly reduced firing of the T6SS apparatus in a *bamA* knockdown strain compared to *tagT* wild-type strain with *bamA* knockdown. These data support the theory that the outer membrane disruption caused by depletion of BamA can generate the signal recognized by the TagQRST-PpkA-FhA1-PppA pathway. However, the actual chemical or physical nature of this signal is not revealed by this experiment.

Disruption of Membrane Biogenesis Can Activate Killing of Nonaggressive Prey by *P. aeruginosa*. Next, we investigated whether knockdown of *bamA* and elevated random assembly and firing of the H1-T6SS organelle could enhance killing of a T6SS$^-$ prey. A *V. cholerae* Δ*vipA* mutant was used for this test because it is not targeted by the tit-for-tat response (42). We performed time-lapse fluorescence microscopy of a coculture of *P. aeruginosa* sg-*bamA* and a *V. cholerae* Δ*vipA* mutant for 1.5 h. We observed that, upon arabinose induction of *dCas9*, *P. aeruginosa* sg-*bamA* was able to kill *V. cholerae* Δ*vipA* (Fig. 7 and Movies S5 and S6) while *P. aeruginosa* sgCTRL and *V. cholerae* Δ*vipA* coexisted without displaying T6SS activity (*SI Appendix*, Fig. S9*A* and Movies S7 and S8) (42). However, this killing did not appear to be targeted in that most of the T6SS$^-$ *V. cholerae* cells that were adjacent to *P. aeruginosa* cells were not killed and these T6SS$^-$ *V. cholerae* even divided and overgrew the field of view over time (Movies S5 and S6). This result suggests that the killing of cells was dependent on their random position rather than the efficient targeting previously observed for T6SS$^+$ *V. cholerae* (42).

Furthermore, the killing events could not be quantified in competition assays (*SI Appendix*, Fig. S10 *A* and *B*), suggesting that the growth rate of the T6SS$^-$ *V. cholerae* strain exceeds the killing rate of prey killing by *P. aeruginosa* activated for H1-T6SS assembly and firing by CRISPRi *bamA* knockdown. The observed killing of *V. cholerae* Δ*vipA* by *P. aeruginosa* sg-*bamA* was T6SS dependent in that a mutant defective in H1-T6SS (sg-*bamA* Δ*vipA*) is unable to kill *V. cholerae* Δ*vipA* (*SI Appendix*, Fig. S9*B* and Movies S9 and S10). We also tested whether *bamA* mRNA was knocked down in *P. aeruginosa* cells that were either positive or negative in the H1-T6SS apparatus. Expression of *bamA* was knocked down to comparable levels in wild-type and the Δ*vipA P. aeruginosa* strains (*SI Appendix*, Fig. S6*A*). Thus, we

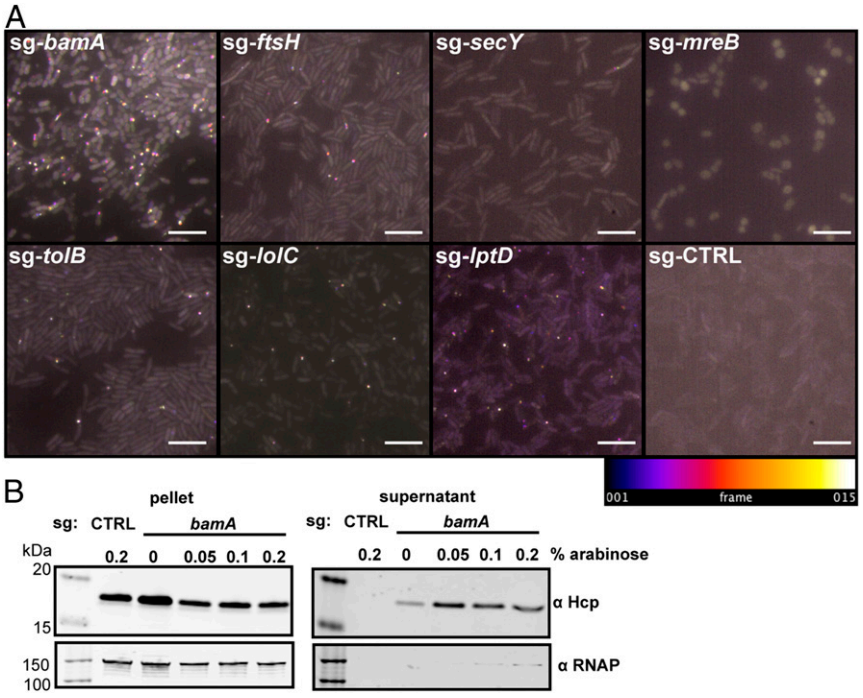

Fig. 5. Knockdown of *bamA* causes dynamic T6SS activation. (*A*) Time-lapse imaging of ClpV-GFP in *P. aeruginosa* strains expressing sgRNA plasmids grown in the presence of 0.1% arabinose. Images were taken every 10 s and temporally color coded. (Scale bar, 10μm.) (*B*) Western blot of Hcp in pellet (*Left*) and supernatant (*Right*) of sg-*bamA* knockdown and sgCTRL. *dCas9* expression was induced with increasing concentrations of arabinose. Cell lysis was controlled by detection of RNAP in the supernatant.

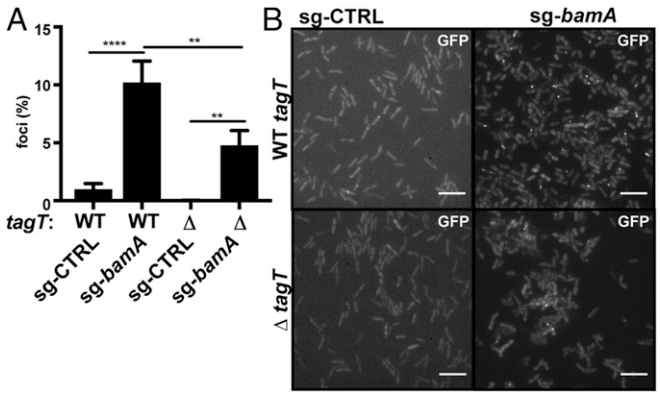

Fig. 6. Membrane stress is signaling via TagQRST to build a functional T6SS apparatus. (*A*) Strains were grown to OD 0.7 to 0.85 in the presence of 0.1% arabinose. T6SS activity of *P. aeruginosa* expressing sg-CTRL and sg-*bamA* plasmids was determined in *P. aeruginosa* wild type and Δ*tagT* by quantifying ClpV-GFP foci in at least 10 different fields of view per individual experiment. Graphs display mean ± SD of three independent experiments. $^{**}P < 0.01$, $^{****}P < 0.0001$. (*B*) Representative image of each strain from *A*. (Scale bar, 10 μm.)

tentatively conclude that membrane stress due to knockdown of *bamA* is sensed by *P. aeruginosa* cells and that these cells then assemble the T6SS apparatus in random locations where the organelles can attack T6SS$^-$ prey cells that by chance are closely adjacent to these sites of H1-T6SS assembly and firing.

Discussion

In this study, we developed a CRISPRi system that works effectively in *P. aeruginosa* PAO1 to target transcriptional downregulation of essential gene expression and then used it to explore the signals that trigger assembly of the H1-T6SS apparatus. The CRISPRi method relies on the RNA guided binding of catalytically inactive Cas9 to the transcription initiation or transcription elongation region of a target gene (67). Specific binding of the sgRNA/dCas9 complex to a target DNA sequence acts as a roadblock to RNA polymerase resulting in reduced transcript levels of the targeted gene. Previously, a different CRISPRi system was developed for *P. aeruginosa*, *Pseudomonas putida*, and *Pseudomonas fluorescens* that relied on a dCas9 derived from *Streptococcus pasteurianus* (71, 84). In the present study, we utilized dCas9 encoded by *Streptococcus pyogenes* that uses an NGG PAM site, compared to the NNGCGA PAM site required by the Cas9 of *S. pasteurianus*. The advantage of the NGG PAM site over the NNGCGA PAM site lies in the higher numbers of potential guides that can be designed for various applications, as the NGG site is less complex and will occur statistically more often than the NNGCGA PAM site. Although the *S. pasteurianus* system has been reported to result in a 10-fold higher gene repression compared to gene knockdown with dCas9 derived from *S. pyogenes* (71, 84), we observed severe growth defects for all our selected essential genes using dCas9 from *S. pyogenes*. Tan et al. also reported that dCas9 from *S. pasteurianus* is less toxic than dCas9 from *S. pyogenes* (84); however, we did not observe any dCas9 toxicity in *P. aeruginosa* PAO1. Furthermore, the two systems are designed with different promoters to drive *dCas9* expression—the Ptet promoter in the *S. pasteurianus* system and the pBAD promoter in our study. The differences in these two CRISPRi systems are thus, in theory, complementary and could allow for their use in combinatorial strategies where independent control of multiple genes might be desired.

The initial goal of our study was to use CRISPRi in *P. aeruginosa* to investigate essential genes whose products reside in the outer membrane (*lptD* and *bamA*), inner membrane (*ftsH* and *secY*), periplasm (*lolC* and *tolB*), and cytosol (*mreB*) in regard to their effects on cell morphology and viability. All knockdowns resulted in severe growth defects and morphological aberrations (the only discordant example being knockdown of *lptD*, which we assume is a nuance associated with pool sizes and turnover of essential products that we decided not to further investigate in the context of this study) (Fig. 2*C*). Transcriptional profiling of *lptD*, *bamA*, and *ftsH* knockdowns revealed up-regulation of various membrane stress responses (*SI Appendix*, Figs. S3 *A–D* and S4 *A* and *B* and Tables S8, S10, and S12). LptD is involved in transport of LPS to the outer leaflet of the outer membrane and has been suggested as a promising vaccine target in other organisms (80) and a drug target in *P. aeruginosa* (85). Upon knockdown of *lptD* we observed an up-regulation in genes involved in lipid A modification, which likely suggests that *P. aeruginosa* cells in this case are trying to compensate for the loss of LPS in their outer membranes by up-regulating other genes involved in LPS biogenesis. The BAM complex is responsible for integrating beta barrel proteins into the gram-negative bacterial outer membrane (56–58, 86–88). Since several OMPs are essential, some components of the BAM complex itself are also essential to gram-negative bacteria. The BAM complex consists of the components BamA–E, where BamA is an essential OMP (57, 87) and BamB–E are lipoproteins anchored to the outer membrane (88–90). In the BAM complex only BamA and BamD are essential (90). Because the BAM complex is required for the integration of the OMP protein LptD, it is not surprising that knockdown of *bamA* also resulted in a similar transcriptional profile compared to the knockdown of *lptD*.

An important result of the present study is that time-lapse microscopy revealed that transcriptional knockdown of *bamA*, *lptD*, and *tolB* through CRISPRi also led to increased dynamic assembly and disassembly of the T6SS apparatus in *P. aeruginosa* (Figs. 3 *A* and *B* and 5*A* and Movies S1 and S4). Surprisingly, knockdown of *ftsH*, *secY*, and *mreB* did not result in increased T6SS dynamic activity. Because cell morphology changes and lysis clearly occur when *ftsH* or *mreB* are knocked down within the same time frames we observe T6SS activation when knocking down transcription of *bamA*, *lptD*, and *tolB* genes, we conclude that the increased T6SS activity seen with knockdown of *bamA* is not likely due to the PARA response (44) and our observed up-regulation of H1-T6SS transcription (Fig. 2*B* and 3 *A* and *B* and *SI Appendix*, Fig. S2 *A–G*). Detection of kin cell lysis is the key tenet of the PARA response which involves the up-regulation of transcription of the genes for T6SS components via the Gac/Rsm/RetS regulatory system but still depends on the TagQRST-PpkA-FhA1-

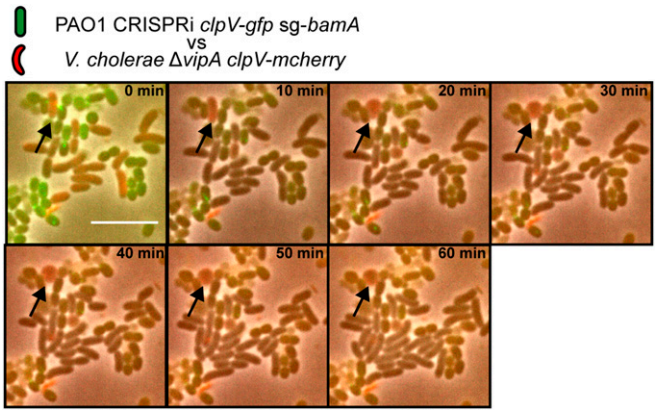

Fig. 7. *P. aeruginosa bamA* knockdown kills T6SS$^-$ *V. cholerae*. Time-lapse imaging of T6SS$^-$ *V. cholerae* 2740-80 ClpV-mCherry2 (1:10 ratio) in mixture with *P. aeruginosa* ClpV-GFP sg-*bamA*. Arrows indicate rounding up of T6SS$^-$ *V. cholerae* after being attacked by *P. aeruginosa*. (Scale bar, 10 μm.)

PppA posttranslational control (44). Because we observed that TagT was required for the observed activation of T6SS after *bamA* knockdown, we conclude that the PARA response does not explain why there is activation of H1-T6SS apparatus assembly and firing after knockdown of *bamA* transcription by CRISPRi.

Previously, LeRoux et al. (44) concluded that TagQRST is not required for T6SS assembly or the TTP response. It is worth noting, however, that these investigators used a *pppA* knockout strain to argue that the TPP pathway is not involved in the PARA response, rather than a knockout of any gene in the *TagQRST* operon (42, 43, 52, 91). Knockout of *pppA*, the gene encoding the phosphatase that opposes PpkA kinase activity, leads to an increase in T6SS apparatus assembly but this strain loses the capacity to respond to an attack by another T6SS$^+$ organism (42, 43). A Δ*pppA* strain of *P. aeruginosa* has been reported to still be capable of killing *B. thailandensis* (44), but this alone is not surprising because of the high level of constitutive random assembly of the H1-T6SS organelle observed in *pppA P. aeruginosa* mutants regardless of whether it is a wild type or a *retS* mutant (42). Measurement of the relative killing activity of *P. aeruginosa* strains against targeted (T6SS$^+$ prey) vs. nontargeted (T6SS$^-$ prey) can also be influenced by factors such as experimental design and multiplicity of infection (42, 44, 45). In this regard, our observation that knockdown of *bamA* activates T6SS in a TagT-dependent fashion is relevant in that such an activated strain can occasionally kill a T6SS$^-$ *V. cholerae* by chance if prey cells are in close proximity to *P. aeruginosa* cells that happen to fire their T6SS in their particular direction (Fig. 7*A* and Movies S5 and S6). Recently, it has also been shown that binding a prey cell to a T6SS$^+$ cell through ligand–receptor interactions can enhance prey cell killing (92). This observation is consistent with the need for high random T6SS activity or, alternatively, adhesin driven cell–cell contact to optimally deploy the T6SS apparatus if the predatory cell lacks an efficient T6SS targeting system such as the TagQRST-PpkA-FhA1-PppA pathway of *P. aeruginosa*. In sum, activation of the T6SS of *P. aeruginosa* can enhance killing of nonaggressive T6SS$^-$ prey cells but the TagQRST-PpkA-FhA1-PppA pathway is needed to detect signals associated with membrane damage (as shown here) or through other cellular envelope insults involving T6SS or T4SS attacks (see below).

The true nature of the signal sensed by the TagQRST-PpkA-FhA1-PppA pathway is unknown, but clearly it can be generated by multiple different insults to the cell envelope of *P. aeruginosa* (36, 42, 43, 51–53, 91, 93). Most recently, an elegant study by Kamal et al. (55) showed that a single effector of *V. cholerae* (TseL) was necessary and sufficient for generating activation of the H1-T6SS of *P. aeruginosa* through the classical tit-for-tat interaction with T6SS$^+$ *V. cholerae.* Ectopic expression of *tseL* in the periplasm of *P. aeruginosa* (but not in the cytosol) could also trigger T6SS assembly in a TagQRST-dependent fashion (55). Given that TseL is a lipase and that lipases are very common effectors of T6SSs (8, 94, 95), it is possible that a signal generated by phospholipid hydrolysis within the periplasm is recognized by part of the *P. aeruginosa* TagQRST sensory transduction system. However, a lipase associated with the T4SS conjugative apparatus has not been identified (96, 97) although other T4SSs do encode putative T4SS lipase effectors and these organisms can also display antibacterial activity (98). Thus, lipid hydrolysis in the *P. aeruginosa* cell envelope may be a universal signal involved in the tit-for-tat response to both aggressive T6SS$^+$ and T4SS$^+$ prey species.

However, the most difficult aspect to imagine in a model where there is a requirement for a T6SS or T4SS lipase effector to generate a signal that is recognized by the TagQRST system of *P. aeruginosa* is the apparent spatial stability of this signal in the context of T6SS tit-for-tat responses (6, 43, 45) and the T6SS dueling phenomena (4). For effectors such as the *V. cholerae* TseL lipase, this might occur via tethering of this effector to the T6SS components that are delivered to the cell (e.g., Hcp-VgrG-PAAR adaptor–effector complexes), especially if such tethering can confine the lipase activity to the site of attack rather than allowing its rapid diffusion in the periplasm or cytosol. Because *P. aeruginosa* can secrete lipase effectors in a T6SS-dependent fashion (8, 11, 95, 99, 100), this model might explain sister cell T6SS dueling despite the presence of T6SS lipase effector immunity proteins. In case immunity proteins are slow to act or are in low abundance in any particular subcellular location where they are delivered by a T6SS exogenous attack by heterologous species or even sister cells of *P. aeruginosa*, the effectors would perform local damage that evokes a T6SS response with enough spatial resolution to fire a response into the same direction from which they received an insult.

In light of the work of Kamal et al. (55), it would seem that the simple puncture of the outer membrane by the T6SS needle is unlikely to be sufficient to elicit a TagQRST-dependent T6SS counterattack for at least *V. cholerae.* Other T6SS$^+$ organisms such as *A. baylyi* undergo tit-for-tat killing by *P. aeruginosa* (42) and also produce a lipase effector but in this case the *A. baylyi* lipase effector is not required for *P. aeruginosa* to detect their functional T6SS and kill this aggressive T6SS$^+$ prey species (45). These results continue to support the idea that membrane disruption can generate a signal at the site of initial T6SS impact depending on the organism that initiates the attack on *P. aeruginosa*. Perhaps T6SS (42, 45) or T4SS (43) attacks that elicit a tit-for-tat response activate a localized lipid hydrolysis event dependent on endogenous periplasmic lipases in *P. aeruginosa*. In this model, such hypothetical lipases could be tethered to stable cell structures (e.g., peptidoglycan) and become activated on encountering T6SS or T4SS attacks and thus provide a quick burst of signal (e.g., hydrolysis products) that can be detected spatially by TagQRST complexes in the vicinity of the attacks. In an analogous way, deletion of outer membrane components by down-regulation of *bamA*, *lptD*, or *tolB* expression could activate the same postulated tethered lipases in such a model. Furthermore, molecules that bind LPS and trigger TagQRST-dependent H1-T6SS activation in *P. aeruginosa* cells such as polymyxin B (24), chelators, and DNA (54) could activate the same postulated lipase molecules. An alternative model postulates that the TagQRST complex could also recognize a localized change in ion fluxes or other signals generated by spatially tethered channels that form spontaneously due to aberrations in lipid structures. Yet another hypothesis suggests that membrane damage changes the distance of the outer membrane to the inner membrane (101–103), which could result in closer proximity of the outer membrane component TagQ and inner membrane components TagST enabling phosphorylation of PpkA and downstream assembly of a T6SS apparatus. A model that incorporates these hypothetical considerations (Fig. 8) provides a framework for future experiments to address the mechanism of these striking responses to interspecies bacterial interactions.

In sum, we designed a CRISPRi system to knock down the expression of essential genes in *P. aeruginosa* and found that depletion of gene products involved in outer membrane biogenesis can generate a signal that triggers T6SS assembly and dynamic activity. These studies shed additional light on the striking T6SS phenomena termed tit-for-tat (42, 43) and T6SS dueling (4) and provide a tool for understanding sensory transduction systems that show spatial and temporal regulation of T6SS assembly such as the TagQRST system of *P. aeruginosa*. Our CRISPRi system for *P. aeruginosa* may also be useful in drug discovery for this challenging nosocomial pathogen (104) given its ability to validate essential gene targets and titrate the

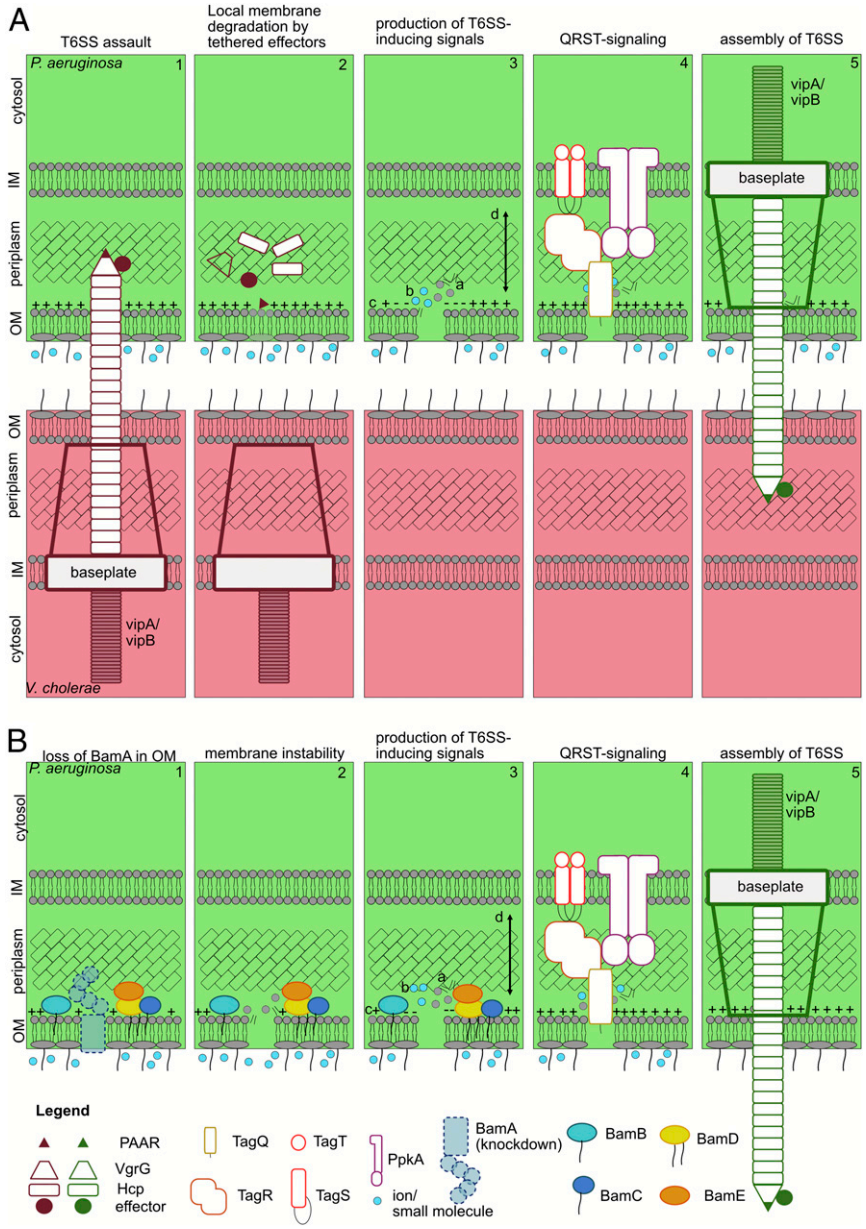

Fig. 8. Model of events that could lead to T6SS firing in *P. aeruginosa*. (*A*) In competition of *V. cholerae and P. aeruginosa*, *V. cholerae* aggressively fires its T6SS apparatus in an unregulated fashion (section 1). Components and effectors of the *V. cholerae* T6SS are locally tethered to the site of attack and the membrane is locally degraded by effectors (section 2). Degradation of the membrane (section 2) could lead to local accumulation of lipid degradation molecules (section 3a), change in local ion or small molecule flux through pore formation (section 3b) or local change in distance between inner membrane (IM) and outer membrane (OM) (section 3c), which could be sensed either directly or indirectly by the TagQRST system leading to phosphorylation of PpkA in the IM (section 4). Phosphorylation of PpkA leads to phosphorylation of FhA and ultimately results in assembly and firing of a *P. aeruginosa* T6SS (section 5). (*B*) Down-regulation of essential genes in the outer membrane (e.g., *bamA*) leads to loss of essential proteins in the OM (1) and destabilization of the OM (section 2). Local membrane destabilization could lead to the same signals locally accumulating in the membrane as in *A* (section 3), resulting in TagQRST signaling (section 4) and assembly of a T6SS (section 5).

expression of their products for validation of drug discovery strategies.

Materials and Methods

Strains and Culture Conditions. *P. aeruginosa* PAO1 and *V. cholerae* 2740-80 were grown in LB (Lysogeny broth - Lennox, 10 mg/L tryptone, 5 g/L yeast extract, 5 g/L sodium chloride) at 37 °C in 15-mL culture tubes overnight. CRISPRi strain culture media were complemented with 30 μg/mL gentamicin to select for the sgRNA plasmid. To induce expression of *dCas9*, 0.2% arabinose was added unless noted differently. Strains used in this study are listed in *SI Appendix*, Table S1. Detailed information on strain construction can be found in the supplemental information.

Growth Curves. Overnight cultures were diluted in LB complemented with 30 μg/mL gentamicin, 0.2% arabinose to an OD_{600} of 0.05, and 150 μL was transferred into a clear 96-well plate in triplicates. Growth at OD_{600} was measured every 30 min in a BioTek Synergy H1 hybrid multimode microplate reader, continuously shaking at 37 °C. Wells containing LB only served as blanks and were subtracted from the data.

qRT-PCRs. RNA was extracted from cultures grown to mid log. Harvested bacteria from 1 mL culture were resuspended in 1 mL TRIzol (Invitrogen) and incubated at room temperature for 5 min, followed by chloroform phase separation. RNA was subsequently purified using the Purelink RNA Mini kit

(Invitrogen). DNase was digested using the Turbo DNA-Free kit (Invitrogen). qRT-PCR was performed using the KAPA SYBR FAST One-Step Universal kit (KAPA Biosystems) on the Eppendorf Mastercycle RealPlex 2 system, following manufacturer's instructions. Primers for gene amplification are listed in *SI Appendix*, Table S2. The mean of the three technical replicates was analyzed in Microsoft Excel v16.27, normalizing to the housekeeping gene *rpsL*. Relative gene expression was calculated after Livak and Schmittgen (105). Three independent experiments were performed. Graphs were generated using GraphPad Prism v7.0b.

Imaging. Overnight cultures were diluted in LB with appropriate antibiotics to OD_{600} of 0.05. *P. aeruginosa* cultures were supplemented with 0.1 or 0.2% arabinose. Cultures were grown to an OD_{600} of 0.7 to 0.85, centrifuged for 5 min at 8,000 × *g*, and resuspended to OD_{600} of 10 in 0.2% arabinose. Agarose pads (1% agarose in either 0.5× Dulbecco's phosphate buffered saline [D-PBS] [Invitrogen] or LB) were prepared and 1 μL bacterial culture was spotted on the pad. Microscope configurations were described previously: Imaging was performed on a Nikon Ti-E inverted motorized microscope with Perfect Focus System and Plan Apo 100× oil Ph3 DM (NA 1.4) objective lens. SPECTRA X light engine (Lumencore), ET-GFP (Chroma 49002) and ET-mCherry (Chroma 49008) filter sets were used to excite and filter fluorescence. To record images, the photometrics CoolSNAP HQ2 camera and NIS Elements 4.0 were used (5). For analysis of the images, ImageJ version 2.0.0-rc69/1.52p was used.

RNA Sequencing. RNAseq libraries were generated as previously described (73). In brief, RNA was extracted using the PureLink RNA mini kit (Invitrogen) and RNAseq libraries were generated following manufacturer's instructions using the Ovation Complete Prokaryotic RNAseq library kit (NuGen). Sequencing was performed on an Illumina NextSeq at Biopolymer's facility at Harvard Medical School. Reads were mapped to the *P. aeruginosa* PAO1 reference genome NC002516. Transcripts per million (TPM) and differential log2 expression values were calculated using the Geneious 11.1.4 software package. Heat maps were generated using Cluster 3.0 and JAVA Treeview version 1.6r4. Volcano plots were generated in Prism 8 version 8.4.3 (471). Principal component analysis (PCA) was performed using Qlucore version 3.6 (27). Data were exported and plots were generated in Prism 8 version 8.4.3 (471) (*SI Appendix*, Fig. S3*D*). Kyoto Encyclopedia of Genes and Genomes (KEGG) pathway analysis was performed using CLC software (*SI Appendix*, Table S8-S13). RNAseq statistics are listed in *SI Appendix*, Table S3.

Hcp Secretion Assays. Overnight cultures were diluted to an OD_{600} of 0.1 in 20 mL LB supplemented with the appropriate antibiotics and different concentrations of inducer in stationary Erlenmeyer flasks to avoid shear stress. Bacteria were harvested and resuspended in 1 mL LB with their respective arabinose concentrations and incubated for 15 min at 37 °C. The pellet and supernatant were collected. The pellet samples were resuspended to 1× Laemmli buffer. Proteins from the supernatant were trichloroacetic acid (TCA) precipitated and resuspended in 1× Laemmli buffer. Western blotting was performed and Hcp and RNAP were detected with the according antibodies.

Flow Cytometry. *P. aeruginosa* strains were grown overnight in LB with 5 μg/mL irgasan and 30 μg/mL gentamicin. Following overnight growth, strains were diluted to a final OD_{600} = 0.05 in LB supplemented with 30 μg/mL gentamicin and 0.2% arabinose and grown at 37 °C for the indicated time points (30 min, 90 min, 3 h, and 5 h). A total of 20 μL of each culture was added to 1 mL D-PBS (Invitrogen) containing 1 μg/mL propidium iodide (Invitrogen) in 5 mL polystyrene tubes (BD Falcon) and allowed to incubate for 15 min in the dark. A total of 100,000 cells for each condition were analyzed by flow cytometry (BD LSRII, 561-nm coherent laser was used for excitation of propidium iodide and emission was detected with a 610/20 bandpass filter) at the Harvard Medical School, Department of Immunology Flow Cytometry Facility. Data were analyzed using FlowJo v10.7.1 software (Treestar).

Statistical Analysis. For statistical analysis, at least three independent experiments were performed in each experiment. One-way ANOVA with subsequent Tukey's multiple comparison test was performed to determine significance. $*P < 0.05$, $**P < 0.01$, $***P < 0.001$, $****P < 0.0001$.

Data Availability. RNAseq data have been deposited in the Gene Expression Omnibus (106) under accession no. GSE159327 (107). All study data are included in the article and *SI Appendix*.

ACKNOWLEDGMENTS. We thank members of the J.J.M. laboratory for helpful discussion and feedback. We thank the Biopolymers Facility Next--Gen Sequencing Core Facility and Department of Immunology Flow Cytometry Facility at Harvard Medical School for their expertise and instrument availability that supported this work. This work was supported by the National Institute of Allergy and Infectious Diseases Grant (AI-26289) (to J.J.M.). A.-S.S. was supported by the Deutsche Forschungsgemeinschaft with the Project STO 1208/1-1.

1. S. Pukatzki *et al.*, Identification of a conserved bacterial protein secretion system in Vibrio cholerae using the Dictyostelium host model system. *Proc. Natl. Acad. Sci. U.S.A.* **103**, 1528–1533 (2006).
2. S. Pukatzki, A. T. Ma, A. T. Revel, D. Sturtevant, J. J. Mekalanos, Type VI secretion system translocates a phage tail spike-like protein into target cells where it cross-links actin. *Proc. Natl. Acad. Sci. U.S.A.* **104**, 15508–15513 (2007).
3. J. D. Mougous *et al.*, A virulence locus of Pseudomonas aeruginosa encodes a protein secretion apparatus. *Science* **312**, 1526–1530 (2006).
4. M. Basler, J. J. Mekalanos, Type 6 secretion dynamics within and between bacterial cells. *Science* **337**, 815 (2012).
5. M. Basler, M. Pilhofer, G. P. Henderson, G. J. Jensen, J. J. Mekalanos, Type VI secretion requires a dynamic contractile phage tail-like structure. *Nature* **483**, 182–186 (2012).
6. B. T. Ho, T. G. Dong, J. J. Mekalanos, A view to a kill: The bacterial type VI secretion system. *Cell Host Microbe* **15**, 9–21 (2014).
7. R. D. Hood *et al.*, A type VI secretion system of Pseudomonas aeruginosa targets a toxin to bacteria. *Cell Host Microbe* **7**, 25–37 (2010).
8. F. Jiang, N. R. Waterfield, J. Yang, G. Yang, Q. Jin, A Pseudomonas aeruginosa type VI secretion phospholipase D effector targets both prokaryotic and eukaryotic cells. *Cell Host Microbe* **15**, 600–610 (2014).
9. F. Boyer, G. Fichant, J. Berthod, Y. Vandenbrouck, I. Attree, Dissecting the bacterial type VI secretion system by a genome wide in silico analysis: What can be learned from available microbial genomic resources? *BMC Genomics* **10**, 104 (2009).
10. A. T. Ma, S. McAuley, S. Pukatzki, J. J. Mekalanos, Translocation of a Vibrio cholerae type VI secretion effector requires bacterial endocytosis by host cells. *Cell Host Microbe* **5**, 234–243 (2009).
11. M. Barret, F. Egan, E. Fargier, J. P. Morrissey, F. O'Gara, Genomic analysis of the type VI secretion systems in Pseudomonas spp.: Novel clusters and putative effectors uncovered. *Microbiology (Reading)* **157**, 1726–1739 (2011).
12. G. Bönemann, A. Pietrosiuk, A. Diemand, H. Zentgraf, A. Mogk, Remodelling of VipA/VipB tubules by ClpV-mediated threading is crucial for type VI protein secretion. *EMBO J.* **28**, 315–325 (2009).
13. Y.-W. Chang, L. A. Rettberg, D. R. Ortega, G. J. Jensen, *In vivo* structures of an intact type VI secretion system revealed by electron cryotomography. *EMBO Rep.* **18**, 1090–1099 (2017).
14. E. Durand *et al.*, Biogenesis and structure of a type VI secretion membrane core complex. *Nature* **523**, 555–560 (2015).
15. M. M. Shneider *et al.*, PAAR-repeat proteins sharpen and diversify the type VI secretion system spike. *Nature* **500**, 350–353 (2013).
16. N. S. Lossi *et al.*, The HsiB1C1 (TssB-TssC) complex of the Pseudomonas aeruginosa type VI secretion system forms a bacteriophage tail sheathlike structure. *J. Biol. Chem.* **288**, 7536–7548 (2013).
17. J. Lopez, P. M. Ly, M. F. Feldman, The tip of the VgrG spike is essential to functional type VI secretion system Assembly in *Acinetobacter baumannii*. *mBio* **11**, e02761-19 (2020).
18. B. S. Weber *et al.*, Genetic dissection of the type VI secretion system in acinetobacter and identification of a novel peptidoglycan hydrolase, TagX, required for its biogenesis. *mBio* **7**, e01253-16 (2016).
19. Y. Cherrak *et al.*, Biogenesis and structure of a type VI secretion baseplate. *Nat. Microbiol.* **3**, 1404–1416 (2018).
20. J. Wang, M. Brodmann, M. Basler, Assembly and subcellular localization of bacterial type VI secretion systems. *Annu. Rev. Microbiol.* **73**, 621–638 (2019).
21. A. Vettiger, J. Winter, L. Lin, M. Basler, The type VI secretion system sheath assembles at the end distal from the membrane anchor. *Nat. Commun.* **8**, 16088 (2017).
22. P. G. Leiman *et al.*, Type VI secretion apparatus and phage tail-associated protein complexes share a common evolutionary origin. *Proc. Natl. Acad. Sci. U.S.A.* **106**, 4154–4159 (2009).
23. M. Kudryashev *et al.*, Structure of the type VI secretion system contractile sheath. *Cell* **160**, 952–962 (2015).
24. A. Zoued *et al.*, Priming and polymerization of a bacterial contractile tail structure. *Nature* **531**, 59–63 (2016).
25. B. J. Burkinshaw *et al.*, A type VI secretion system effector delivery mechanism dependent on PAAR and a chaperone-co-chaperone complex. *Nat. Microbiol.* **3**, 632–640 (2018).
26. D. Unterweger *et al.*, Chimeric adaptor proteins translocate diverse type VI secretion system effectors in Vibrio cholerae. *EMBO J.* **34**, 2198–2210 (2015).
27. X. Liang *et al.*, Identification of divergent type VI secretion effectors using a conserved chaperone domain. *Proc. Natl. Acad. Sci. U.S.A.* **112**, 9106–9111 (2015).
28. S. Koskiniemi *et al.*, Rhs proteins from diverse bacteria mediate intercellular competition. *Proc. Natl. Acad. Sci. U.S.A.* **110**, 7032–7037 (2013).

29. J. M. Silverman *et al*., Haemolysin coregulated protein is an exported receptor and chaperone of type VI secretion substrates. *Mol. Cell* **51**, 584–593 (2013).
30. E. Durand *et al*., Crystal structure of the VgrG1 actin cross-linking domain of the Vibrio cholerae type VI secretion system. *J. Biol. Chem.* **287**, 38190–38199 (2012).
31. A. Hachani *et al*., Type VI secretion system in Pseudomonas aeruginosa: Secretion and multimerization of VgrG proteins. *J. Biol. Chem.* **286**, 12317–12327 (2011).
32. T. E. Wood *et al*., The Pseudomonas aeruginosa T6SS delivers a periplasmic toxin that disrupts bacterial cell morphology. *Cell Rep.* **29**, 187–201.e7 (2019).
33. P. Pissaridou *et al*., The *Pseudomonas aeruginosa* T6SS-VgrG1b spike is topped by a PAAR protein eliciting DNA damage to bacterial competitors. *Proc. Natl. Acad. Sci. U.S.A.* **115**, 12519–12524 (2018).
34. A. Hachani, L. P. Allsopp, Y. Oduko, A. Filloux, The VgrG proteins are "à la carte" delivery systems for bacterial type VI effectors. *J. Biol. Chem.* **289**, 17872–17884 (2014).
35. A. B. Russell *et al*., Type VI secretion delivers bacteriolytic effectors to target cells. *Nature* **475**, 343–347 (2011).
36. F. Hsu, S. Schwarz, J. D. Mougous, TagR promotes PpkA-catalysed type VI secretion activation in Pseudomonas aeruginosa. *Mol. Microbiol.* **72**, 1111–1125 (2009).
37. J. D. Mougous, C. A. Gifford, T. L. Ramsdell, J. J. Mekalanos, Threonine phosphorylation post-translationally regulates protein secretion in Pseudomonas aeruginosa. *Nat. Cell Biol.* **9**, 797–803 (2007).
38. J. A. Moscoso, H. Mikkelsen, S. Heeb, P. Williams, A. Filloux, The Pseudomonas aeruginosa sensor RetS switches type III and type VI secretion via c-di-GMP signalling. *Environ. Microbiol.* **13**, 3128–3138 (2011).
39. A. L. Goodman *et al*., A signaling network reciprocally regulates genes associated with acute infection and chronic persistence in Pseudomonas aeruginosa. *Dev. Cell* **7**, 745–754 (2004).
40. A. L. Goodman *et al*., Direct interaction between sensor kinase proteins mediates acute and chronic disease phenotypes in a bacterial pathogen. *Genes Dev.* **23**, 249–259 (2009).
41. I. Ventre *et al*., Multiple sensors control reciprocal expression of Pseudomonas aeruginosa regulatory RNA and virulence genes. *Proc. Natl. Acad. Sci. U.S.A.* **103**, 171–176 (2006).
42. M. Basler, B. T. Ho, J. J. Mekalanos, Tit-for-tat: Type VI secretion system counterattack during bacterial cell-cell interactions. *Cell* **152**, 884–894 (2013).
43. B. T. Ho, M. Basler, J. J. Mekalanos, Type 6 secretion system-mediated immunity to type 4 secretion system-mediated gene transfer. *Science* **342**, 250–253 (2013).
44. M. LeRoux *et al*., Kin cell lysis is a danger signal that activates antibacterial pathways of Pseudomonas aeruginosa. *eLife* **4**, e05701 (2015).
45. P. D. Ringel, D. Hu, M. Basler, The role of type VI secretion system effectors in target cell lysis and subsequent horizontal gene transfer. *Cell Rep.* **21**, 3927–3940 (2017).
46. T. M. Brooks, D. Unterweger, V. Bachmann, B. Kostiuk, S. Pukatzki, Lytic activity of the Vibrio cholerae type VI secretion toxin VgrG-3 is inhibited by the antitoxin TsaB. *J. Biol. Chem.* **288**, 7618–7625 (2013).
47. T. G. Dong, B. T. Ho, D. R. Yoder-Himes, J. J. Mekalanos, Identification of T6SS-dependent effector and immunity proteins by Tn-seq in Vibrio cholerae. *Proc. Natl. Acad. Sci. U.S.A.* **110**, 2623–2628 (2013).
48. G. English *et al*., New secreted toxins and immunity proteins encoded within the Type VI secretion system gene cluster of Serratia marcescens. *Mol. Microbiol.* **86**, 921–936 (2012).
49. A. Brencic, S. Lory, Determination of the regulon and identification of novel mRNA targets of Pseudomonas aeruginosa RsmA. *Mol. Microbiol.* **72**, 612–632 (2009).
50. A. Brencic *et al*., The GacS/GacA signal transduction system of Pseudomonas aeruginosa acts exclusively through its control over the transcription of the RsmY and RsmZ regulatory small RNAs. *Mol. Microbiol.* **73**, 434–445 (2009).
51. J. M. Silverman *et al*., Separate inputs modulate phosphorylation-dependent and -independent type VI secretion activation. *Mol. Microbiol.* **82**, 1277–1290 (2011).
52. M. G. Casabona *et al*., An ABC transporter and an outer membrane lipoprotein participate in posttranslational activation of type VI secretion in Pseudomonas aeruginosa. *Environ. Microbiol.* **15**, 471–486 (2013).
53. J. D. Mougous, C. A. Gifford, T. L. Ramsdell, J. J. Mekalanos, Threonine phosphorylation post-translationally regulates protein secretion in *Pseudomonas aeruginosa*. *Nat. Cell Biol.* **9**, 797–803 (2007).
54. M. Wilton *et al*., Chelation of membrane-bound cations by extracellular DNA activates the type VI secretion system in Pseudomonas aeruginosa. *Infect. Immun.* **84**, 2355–2361 (2016).
55. F. Kamal *et al*., Differential cellular response to translocated toxic effectors and physical penetration by the type VI secretion system. *Cell Rep.* **31**, 107766 (2020).
56. C. Pinto *et al*., Formation of the β-barrel assembly machinery complex in lipid bilayers as seen by solid-state NMR. *Nat. Commun.* **9**, 4135 (2018).
57. D. Gessmann *et al*., Outer membrane β-barrel protein folding is physically controlled by periplasmic lipid head groups and BamA. *Proc. Natl. Acad. Sci. U.S.A.* **111**, 5878–5883 (2014).
58. D. Ni *et al*., Structural and functional analysis of the β-barrel domain of BamA from Escherichia coli. *FASEB J.* **28**, 2677–2685 (2014).
59. R. Haarmann, M. Ibrahim, M. Stevanovic, R. Bredemeier, E. Schleiff, The properties of the outer membrane localized Lipid A transporter LptD. *J. Phys. Condens. Matter* **22**, 454124 (2010).
60. A. Lo Sciuto *et al*., The periplasmic protein TolB as a potential drug target in Pseudomonas aeruginosa. *PLoS One* **9**, e103784 (2014).
61. R. Lloubès *et al*., The Tol-Pal proteins of the Escherichia coli cell envelope: An energized system required for outer membrane integrity? *Res. Microbiol.* **152**, 523–529 (2001).
62. S. Carr, C. N. Penfold, V. Bamford, R. James, A. M. Hemmings, The structure of TolB, an essential component of the tol-dependent translocation system, and its protein-protein interaction with the translocation domain of colicin E9. *Structure* **8**, 57–66 (2000).
63. M. Jinek *et al*., A programmable dual-RNA-guided DNA endonuclease in adaptive bacterial immunity. *Science* **337**, 816–821 (2012).
64. F. A. Ran *et al*., Genome engineering using the CRISPR-Cas9 system. *Nat. Protoc.* **8**, 2281–2308 (2013).
65. H. Wang *et al*., One-step generation of mice carrying mutations in multiple genes by CRISPR/Cas-mediated genome engineering. *Cell* **153**, 910–918 (2013).
66. L. S. Qi *et al*., Repurposing CRISPR as an RNA-guided platform for sequence-specific control of gene expression. *Cell* **152**, 1173–1183 (2013).
67. M. H. Larson *et al*., CRISPR interference (CRISPRi) for sequence-specific control of gene expression. *Nat. Protoc.* **8**, 2180–2196 (2013).
68. I. S. Myrbråten *et al*., CRISPR interference for rapid knockdown of essential cell cycle genes in *Lactobacillus plantarum*. *mSphere* **4**, e00007-19 (2019).
69. D. Bikard *et al*., Programmable repression and activation of bacterial gene expression using an engineered CRISPR-Cas system. *Nucleic Acids Res.* **41**, 7429–7437 (2013).
70. E. Choudhary, P. Thakur, M. Pareek, N. Agarwal, Gene silencing by CRISPR interference in mycobacteria. *Nat. Commun.* **6**, 6267 (2015).
71. J. M. Rock *et al*., Programmable transcriptional repression in mycobacteria using an orthogonal CRISPR interference platform. *Nat. Microbiol.* **2**, 16274 (2017).
72. X. Liu *et al*., High-throughput CRISPRi phenotyping identifies new essential genes in *Streptococcus pneumoniae*. *Mol. Syst. Biol.* **13**, 931 (2017).
73. F. Caro, N. M. Place, J. J. Mekalanos, Analysis of lipoprotein transport depletion in *Vibrio cholerae* using CRISPRi. *Proc. Natl. Acad. Sci. U.S.A.* **116**, 17013–17022 (2019).
74. R. Voulhoux, M. P. Bos, J. Geurtsen, M. Mols, J. Tommassen, Role of a highly conserved bacterial protein in outer membrane protein assembly. *Science* **299**, 262–265 (2003).
75. H. Dong *et al*., Structural basis for outer membrane lipopolysaccharide insertion. *Nature* **511**, 52–56 (2014).
76. S. Qiao, Q. Luo, Y. Zhao, X. C. Zhang, Y. Huang, Structural basis for lipopolysaccharide insertion in the bacterial outer membrane. *Nature* **511**, 108–111 (2014).
77. T. Ogura *et al*., Balanced biosynthesis of major membrane components through regulated degradation of the committed enzyme of lipid A biosynthesis by the AAA protease FtsH (HflB) in Escherichia coli. *Mol. Microbiol.* **31**, 833–844 (1999).
78. T. Tomoyasu *et al*., The Escherichia coli FtsH protein is a prokaryotic member of a protein family of putative ATPases involved in membrane functions, cell cycle control, and gene expression. *J. Bacteriol.* **175**, 1344–1351 (1993).
79. Y. Akiyama, T. Ogura, K. Ito, Involvement of FtsH in protein assembly into and through the membrane. I. Mutations that reduce retention efficiency of a cytoplasmic reporter. *J. Biol. Chem.* **269**, 5218–5224 (1994).
80. Z. Zha, C. Li, W. Li, Z. Ye, J. Pan, LptD is a promising vaccine antigen and potential immunotherapeutic target for protection against *Vibrio* species infection. *Sci. Rep.* **6**, 38577 (2016).
81. J. C. Malinverni *et al*., YfiO stabilizes the YaeT complex and is essential for outer membrane protein assembly in Escherichia coli. *Mol. Microbiol.* **61**, 151–164 (2006).
82. A. Hinz, S. Lee, K. Jacoby, C. Manoil, Membrane proteases and aminoglycoside antibiotic resistance. *J. Bacteriol.* **193**, 4790–4797 (2011).
83. J. D. Mills, Y. Kawahara, M. Janitz, Strand-specific RNA-seq provides greater resolution of transcriptome profiling. *Curr. Genomics* **14**, 173–181 (2013).
84. S. Z. Tan, C. R. Reisch, K. L. J. Prather, A robust CRISPR interference gene repression system in Pseudomonas. *J. Bacteriol.* **200**, e00575-17 (2018).
85. N. Srinivas *et al*., Peptidomimetic antibiotics target outer-membrane biogenesis in Pseudomonas aeruginosa. *Science* **327**, 1010–1013 (2010).
86. N. Noinaj *et al*., Structural insight into the biogenesis of β-barrel membrane proteins. *Nature* **501**, 385–390 (2013).
87. A. M. Plummer, K. G. Fleming, From chaperones to the membrane with a BAM! *Trends Biochem. Sci.* **41**, 872–882 (2016).
88. T. Wu *et al*., Identification of a multicomponent complex required for outer membrane biogenesis in Escherichia coli. *Cell* **121**, 235–245 (2005).
89. J. G. Sklar *et al*., Lipoprotein SmpA is a component of the YaeT complex that assembles outer membrane proteins in Escherichia coli. *Proc. Natl. Acad. Sci. U.S.A.* **104**, 6400–6405 (2007).
90. C. Onufryk, M.-L. Crouch, F. C. Fang, C. A. Gross, Characterization of six lipoproteins in the sigmaE regulon. *J. Bacteriol.* **187**, 4552–4561 (2005).
91. D. Liebl, M. Robert-Genthon, V. Job, V. Cogoni, I. Attrée, Baseplate component TssK and spatio-temporal assembly of T6SS in Pseudomonas aeruginosa. *Front. Microbiol.* **10**, 1615 (2019).
92. S.-Y. Ting *et al*., Targeted depletion of bacteria from mixed populations by programmable adhesion with antagonistic competitor cells. *Cell Host Microbe* **28**, 313–321.e6 (2020).
93. L. Lin, E. Lezan, A. Schmidt, M. Basler, Abundance of bacterial Type VI secretion system components measured by targeted proteomics. *Nat. Commun.* **10**, 2584 (2019).
94. B. T. Ho, Y. Fu, T. G. Dong, J. J. Mekalanos, *Vibrio cholerae* type 6 secretion system effector trafficking in target bacterial cells. *Proc. Natl. Acad. Sci. U.S.A.* **114**, 9427–9432 (2017).
95. S. Wettstadt, T. E. Wood, S. Fecht, A. Filloux, Delivery of the Pseudomonas aeruginosa phospholipase effectors PldA and PldB in a VgrG- and H2-T6SS-dependent manner. *Front. Microbiol.* **10**, 1718 (2019).

96. J. E. Gordon *et al*., Use of chimeric type IV secretion systems to define contributions of outer membrane subassemblies for contact-dependent translocation. *Mol. Microbiol.* **105**, 273–293 (2017).
97. P. J. Christie, The mosaic type IV secretion systems. *Ecosal Plus*, 10.1128/ecosalplus.ESP-0020-2015 (2016).
98. D. P. Souza *et al*., Bacterial killing via a type IV secretion system. *Nat. Commun.* **6**, 6453 (2015).
99. T. E. Wood, S. A. Howard, S. Wettstadt, A. Filloux, PAAR proteins act as the 'sorting hat' of the type VI secretion system. *Microbiology (Reading)* **165**, 1203–1218 (2019).
100. A. B. Russell *et al*., Diverse type VI secretion phospholipases are functionally plastic antibacterial effectors. *Nature* **496**, 508–512 (2013).
101. S. I. Miller, N. R. Salama, The gram-negative bacterial periplasm: Size matters. *PLoS Biol.* **16**, e2004935 (2018).
102. A. T. Asmar *et al*., Communication across the bacterial cell envelope depends on the size of the periplasm. *PLoS Biol.* **15**, e2004303 (2017).
103. C. M. Oikonomou, G. J. Jensen, Cellular electron cryotomography: Toward structural biology in situ. *Annu. Rev. Biochem.* **86**, 873–896 (2017).
104. K. E. R. Bachta, J. P. Allen, B. H. Cheung, C.-H. Chiu, A. R. Hauser, Systemic infection facilitates transmission of Pseudomonas aeruginosa in mice. *Nat. Commun.* **11**, 543 (2020).
105. K. J. Livak, T. D. Schmittgen, Analysis of relative gene expression data using real-time quantitative PCR and the 2(-Δ Δ C(T)) Method. *Methods* **25**, 402–408 (2001).
106. R. Edgar, M. Domrachev, A. E. Lash, Gene expression Omnibus: NCBI gene expression and hybridization array data repository. *Nucleic Acids Res.* **30**, 207–210 (2002).
107. A.-S. Stolle, J. J. Mekalanos, CRISPRi knockdown of essential genes in *Pseudomonas aeruginosa. Gene Expression Omnibus* (GEO). http://www.ncbi.nlm.nih.gov/geo/query/acc.cgi?acc=GSE159327. Deposited 9 October 2020.